

Effects of Cloud Cover Variations, El Niño and the North Atlantic Oscillation on Thermal Potential

A. Tokgozlu

Süleyman Demirel University, Faculty of Science

Isparta, Türkiye

tokgozlu@fef.sdu.edu.tr

Z. Aslan

Beykoz Logistics School of Higher Education

Kavacak, Istanbul, Türkiye

zaferaslan@beykoz.edu.tr

Abstract

This paper analyzes the role of climatological variations and effects of El Niño, La Nina and the North Atlantic Oscillation (NAO) on cloud cover and the role of cloud cover on thermal potential in selected areas in Turkey. Positive anomalies in the NAO and the strongest La Nina years (weakest El Niño years) correspond with decreasing trends of cloud cover values (increasing probability of dry thermals). This study utilizes 1D wavelet packets and continuous wavelets on historical cloud cover values in northwestern and central parts of Turkey. The results show a role of cloud cover variations on thermal structure and soaring potential of the study area over last 35 years and favorable soaring conditions with wet thermals in the next decade.

Nomenclature

a	=	scaling parameter
b	=	location parameter
C ψ	=	admissibility condition
f	=	single function, mother wavelet (cloud cover)
F	=	Fourier transform
h	=	altitude of station
W _f (a,b)	=	wavelet transform
W(a)	=	wavelet variance
$\psi(t)$	=	continuous wavelet

Introduction

Olofsson and his group describe a technique to define the thermal height and the lowest value of the top of dry thermals and cumulus cloud base.¹ Additionally, weather predictions have been evaluated using glider flight data by determining convective boundary layer (CBL) depth, glider climb rates, wind velocity at 1000m above mean-sea-level (msl) and the onset of convective clouds.² For thermal forecasting, sensible heat flux, terrain characteristics, temperature advection, wind velocity and cloud cover are listed as important variables.

The purpose of wavelet analysis is to find out the cluster pattern of smooth versions of variables. Wavelet techniques which have been commonly used in engineering problems in recent years are an alternative method to the Fast Fourier Transform (FFT) algorithm. Functions can be approximated to any prescribed accuracy with a finite sum of wavelet transforms. The wavelet transform decomposes a signal into a set of special basis functions that are wavelet functions. The wavelet expansion gives a time and frequency localization of the signal. This specification means that most of the energy of the signal is well represented by a few sets of wavelet basis functions. This can help in

signal identification. After several introductions to apply wavelets in monthly and annual variations of cloud cover data in the central Anatolia (Isparta) and Marmara (Eskişehir) regions of Turkey, small-, meso- and large-scale effects on fluctuations have been demonstrated.^{3, 4} Wavelet analyses helps to explain cross interactions between variables. Results of this paper can be used to determine changes in climate, thermal potential and the roles of El Niño and the NAO.

Material and methods

The study area covers climatological stations in the Central Anatolia and Marmara regions of Turkey. Monthly and annual average values of cloud cover between 1970 and 2007 were analyzed for Kandilli (Istanbul; 40°55' N, 29°05' E, h = 114m above msl), Eskişehir (39° 30' N, 30° 31' E, h = 800m above msl) and Isparta (37°46' N, 30°33' E, h = 997m above msl), see Fig. 1. Cloud cover values are recorded based on recorded hourly meteorological observations. Cloud cover values range between 0-10 with 0 corresponding to clear conditions and 10 corresponding to overcast conditions.

Wavelet techniques

This study is based on wavelet techniques and their applications to cloud cover data. In this section we give the basic definitions about the wavelet transform. Wavelets are families of small waves generated from a single function $f(t)$ which is called the mother wavelet. A sufficient condition for $f(t)$ to qualify as a mother wavelet is given as below:^{3,4}

$$\int_{-\infty}^{\infty} |f(t)|^2 dt < \infty \quad (1a)$$

The Fourier transform F of $f(t)$ is defined as

$$F(w) = \int_{-\infty}^{\infty} f(t)e^{iwt} dt \quad (1b)$$

A function $\psi(t)$ satisfying the following condition is called a continuous wavelet:

$$\int_{-\infty}^{\infty} |\psi(t)|^2 dt = 1 \quad (2a)$$

and

$$\int_{-\infty}^{\infty} \psi(t) dt = 0 \quad (2b)$$

Higher order moments may be zero, that is,

$$\int_{-\infty}^{\infty} t^k \psi(t) dt = 0 \quad \text{for } k = 0, \dots, N-1$$

The wavelet transform of $f(t)$ denoted by $W_f(a,b)$ is defined as:

$$W_f(a,b) = \frac{1}{\sqrt{a}} \int_{-\infty}^{\infty} \psi((u-b)/a) f(u) du = \int_{-\infty}^{\infty} f(u) \psi_{a,b}^{(u)} du \quad (3)$$

$$\text{Where } \psi_{a,b}^{(u)} = \frac{1}{\sqrt{a}} \psi((u-b)/a) \quad (4)$$

Here a is a scaling parameter, b is a location parameter and $\psi_{a,b}^{(u)}$ is often called continuous wavelet (or daughter wavelet) while $\psi(u)$ is the mother wavelet. If $\psi_{j,k}^{(u)} = 2^j \psi(2^j u - k)$ is an orthonormal system, that is;

$$\int_{-\infty}^{\infty} \psi_{j,k}^{(u)} \psi_{m,n}^{(u)} du = \delta_{j,m} \delta_{k,n} \quad (5)$$

then ψ is a wavelet and the admissibility condition

$$C_\psi = 2\pi \int_{-\infty}^{\infty} |\psi(w)|^2 / w dw < \infty \quad (6)$$

is satisfied.

The term $|W_f(a,b)|^2$ is called the scalogram of the function f and it can also be interpreted as energy density:⁵

$$\int_{-\infty}^{\infty} |W_f(a,b)|^2 db = W(a) \quad (7)$$

This is called the wavelet variance or wavelet spectrum. It may be observed that the scalogram can be represented either as three-dimensional plot or as a two-dimensional grey scale image.⁶ As mentioned above, parameters a and b represent, respectively, the scaling factor and the location in time.⁷ In the following sections, $f(t)$ will be considered as monthly or annual average values of cloud cover over selected areas in Turkey.

Table 1 presents definitions of climate variability and the related time scale values in months or in years. In this paper, by applying wavelet techniques, climate variability (role of inter-monthly fluctuations, semi-annual cycle, residual annual

cycle, inter-annual variations, sub-decadal variations, decadal to centennial changes) on cloud cover variations and its local time will be defined.

Analysis

This section covers analysis of cloud cover data and wavelet technique applications.

Variation of monthly and annual average cloud cover values

Figures 2a and 2b show temporal variations of monthly cloud cover values in Eskişehir. In recent years, cloud cover values have a statistically insignificant decreasing trend ($R^2 \sim 0$). The striking feature of the two figures is the periodic nature of the cloud cover; a minimum in the summer months (less than 2) and a maximum in the winter months (more than 6). The periodicity is best illustrated in Fig. 2a.

Figures 2c and 2d present 1D wavelet and continuous wavelet analyses of cloud cover values observed in Eskişehir, between 1982 and 2007. Actual variation (a_3) of cloud cover data and detailed variation at level 3 (d_3) are smaller in the middle part of the study period. Annual cycle (1.3-16 month) of cloud cover values and large scale effects on this variation can be observed in the figures. But, in 1990, 1998 and 2007, in general, small- and meso-scale fluctuations play an important role in these cloud cover values (scales vary from minimum to maximum, from dark to light). In the strongest El Niño years (1982-1983, 1986-1987, 1991-1992, 1997-1998) larger cloud cover values were observed. In the strongest La Nina years (1998-1999, 1988-1989, 1975-1976, 1970-1971) smaller cloud cover values were recorded.⁸

Figure 3a presents annual variations of cloud cover data between 1975 and 2006 in Isparta (approximately 100km away from Antalya towards the North). In general, until the 1990's the largest decreasing trend was observed. Statistical analysis shows a statistically significant decreasing trend through the entire observation period; the linear correlation R^2 value was 0.50.

Figures 3b and 3c represent wavelet analyses of the cloud cover data from Isparta. In the first part of study period, standard deviation values were larger than the values observed in the second part. In all periods, large- and meso-scale fluctuations play an important role as seen by the frequency changes between 1 and 61 months, (Fig. 3b, vertical axis). But, meso-scale fluctuations on the cloud cover values were more active in between 1990-1992 and 1996-1998. It may be important that these periods coincided with El Niño years.⁸

Figure 4 shows annual temporal variations of cloud cover values in Istanbul (Kandilli), ($R^2 = 0.05$). The variations have a similar decreasing trend of cloud cover values as observed in Eskişehir and Isparta; only the trend in Isparta is statistically significant ($\alpha = 0.01$). Similarly, small-, meso- and large-scale effects on cloud cover were detected at and near the vicinity of Kandilli (Figs. 4c and 4d).

Analysis of the North Atlantic Oscillation effects

The NAO is a climatic phenomenon in the North Atlantic Ocean of fluctuations in the difference of atmospheric pressure at sea-level between the Icelandic Low and the Azores High.⁹ Through east-west oscillation motions of the Icelandic Low and the Azores High, it controls the strength and direction of westerly winds and storm tracks across the North Atlantic. It is highly correlated with the Arctic Oscillation, as the Arctic oscillation is a part of the NAO. The NAO was discovered in the 1920s by Sir Gilbert Walker. Unlike the El Niño phenomenon in the Pacific Ocean, the NAO is a larger atmospheric event. It is one of the most important manifestations of climate fluctuations in the North Atlantic and surrounding humid climates.

The positive phase of the NAO reflects below-normal heights and pressure across the high latitudes of the North Atlantic and above-normal heights and pressure over the central North Atlantic, the eastern United States and western Europe. Strong positive phases of the NAO tend to be associated with below-average temperatures in Greenland and often across southern Europe and the Middle East. Positive phases are also associated with below-average precipitation over southern and central Europe. Opposite patterns of temperature and precipitation anomalies are typically observed during strong negative phases of the NAO.

Analysis of the NAO temporal variations between 1950 and 2006 are presented in Fig. 5a. Additionally, in Fig. 3a, it can be seen that between 1985 and 1990 and, between 1992 and 2006 the cloud cover values in Isparta were smaller than the other part of the period. It can be seen in Fig. 5a that NAO z-score (normalized value: (monthly average – long term average) / standard deviation) fluctuations showed more positive anomalies beginning from 1990's. Positive NAO anomalies were accompanied by lower cloud observations in study area. As a result, positive NAO anomalies may result in decreasing values of cloud cover and precipitation in western Anatolia.

As can be seen in Figs. 3b and 3c, meso- and large-scale effects were observed in Isparta between 1982-1983 and 1987-1988. Large-scale fluctuations, inter-annual and sub-decadal variations (5-61 months, Table 1) occurred between 1997 and 2002, (Fig. 5d). Thus, the lowest cloud cover values are accompanied by positive NAO values.

Seasonal analyses of cloud cover values

Figures 6a through 6h show the variation of cloud cover values in Eskişehir between 1982 and 2006 and the corresponding NAO values in four seasons. Linear correlation between annual average NAO and cloud cover values in Eskişehir and Isparta are presented in Fig. 6i and 6j. These correlations are significant with a significant level of $\alpha = 0,10$. The correlation is more significant in Eskişehir than Isparta.

Decreasing trends are apparent in cloud cover and NAO values in spring, summer and winter in Eskişehir. However, in autumn the trends are the opposite; the cloud cover values show a slightly increasing trend. There is a negative linear relation ($R^2 = 0.14$) between cloud cover and NAO: increasing NAO

values correspond to decreasing cloud cover values. This relation has to be analyzed in more detail in further studies.

These results suggest the following effects on soaring conditions in the study area in the near future.¹⁰ If the NAO values continue to increase over the study area it is concluded that more dry thermals will be observed in spring and summer, but more wet thermals in autumn.

Results and conclusion

The purpose of this study was to investigate the large scale effects of El Niño and the North Atlantic Oscillations (NAO) on cloud cover variations in the northwestern and central part of Turkey. For this purpose, monthly and annual cloud cover values were analyzed.

A unique wavelet analysis was performed on the cloud cover data. The wavelet toolbox contains graphical tools available to examine and explore properties of individual wavelets and wavelet packets. Wavelet analysis examines statistics of signals and signal components. A continuous wavelet transform of a one-dimensional signal performs discrete analysis and synthesis of one- and two-dimensional features. The wavelet map is a graphical representation of the function (sometimes called the wavelet coefficients) of two variables and for a given wavelet. Large values of the function (the so-called wavelet coefficients) reflect the combined effects of a large fluctuation of the signal f at this time and of a good matching of shape between the signal and the wavelet. It should be noted that the wavelet function isolates local minima and maxima of the signal at the selected duration. In some applications, the presence of a 'bump' in a signal may be more significant than its size. Then, it is imperative to display a local maximum.

From the wavelet analyses of the cloud cover, El Niño and NAO data we learned the following:

- Local maximum lines are presented in wavelet analysis of cloud cover values with 1D continuous wavelet analysis.
- 1D continuous wavelet analyses present results in time and frequency domains on the same graph. Inter monthly (time scale: 2.0-3.1 months) and annual (1.3-16.0 months) cycles of cloud cover data, amplitudes and deviations of signal are interpreted with 1D wavelet analysis. Comparing Figs. 2d and 3c, it is clear that there was large power in the 1-5 year cloud cover period during both the earlier and latter parts of this century. In addition, there are 1-4 year and 1-5 year oscillations in Eskişehir and Isparta, respectively. The wavelet analyses give information on changes in frequency that may have occurred. For example, at Isparta, cloud cover variations have undergone a slower oscillation than at Eskişehir.
- Continuous wavelet analysis of NAO z-scores explains local maximum values, sub-decadal (5.3-8.3 years) variations and decadal changes (more than 10.6 years). In the figures showing the z-scores, the x -axis is the wavelet location in time and the y -axis is the wavelet period in years. The red areas indicate that large scale

effects (*Editor's note: color depicted in the on-line version*). The inter-decadal fluctuations have the effect of modulating the amplitude and frequency of occurrence of NAO events.

Buoyancy results from surface heating. But if convective clouds are present, then additional buoyancy will be released aloft through the latent heat of condensation. By considering monthly average values of cloud cover in this study, no distinction is made between low-, middle-, or high-level clouds. Convective clouds mark thermals, but they also add buoyancy to the thermals through the latent heat of condensation. Also, with cloud formation the maximum height is reached to which a glider can climb. Because cloud-generated buoyancy is so significant, the best soaring conditions often occur when clouds form. Minimum thermalling conditions are available in the absence of clouds. Forming overcast blocks sunlight from reaching the surface, reduces the surface buoyancy and weakens the thermals.

In the strongest El Niño years, monthly average cloud cover values are higher than long term mean values. Thus, with the previous buoyancy factors in mind, these conditions are associated with organization of more wet thermals for soaring. But, in the strong La Nina years, the occurrence of more dry thermals is expected.

Long term data (1950-2006) shows positive and negative relations between cloud cover values and NAO variations in different seasons. The results show that there is a negative relation between NAO and annual average cloud cover values in the study area: increasing positive NAO values correspond to decreasing cloud cover values and decreasing positive NAO values correspond to increasing cloud cover values. Further, the increasing cloud cover values are higher in autumn.

These results suggest the following effects on soaring conditions over the study area assuming the NAO values continue to decrease in the next decade. In spring and summer more dry thermals are expected but more wet thermals are expected in autumn.

References

- ¹Olofsson, B. and Olsson, E., "Automatic thermal forecast from the Swedish HIRLAM", Technical Soaring, Vol. 30, No: 4, pp. 101-104, 2006.
- ²Hindman, E., "Evaluating Weather Predictions using Glider Flights, Fall 2006 and Spring 2007 Pennsylvania, USA", Workshop of OSTIV Meteorological Panel, 24-30 Sept., 2007.
- ³Meyer, Y., "The role of oscillation in some nonlinear problems", School on Mathematical Problems in Image Processing, ICTP, SMR 1237/4, pp. 4-22, 2000.
- ⁴Can, Z., Aslan, Z. and Oguz, O., "One-dimensional wavelet and re-analysis of gravity waves", The Arabian Journal for Science and Engineering, Vol. 29, No. 2C, pp. 33-42, 2004.
- ⁵Can, Z., Aslan, Z., Oguz, O. and Siddiqi, A., "Wavelet transforms of meteorological parameters and gravity waves", Annals Geophysics, Vol. 23, pp. 650-663, 2005.

⁶Siddiqi, A., Aslan, Z. and Tokgozlu, A., "Wavelet based computer simulation of some meteorological parameters: Case study in Turkey", Trends in Industrial and Applied Mathematics. H. Siddiqi and M. Kocvara (Editors), pp. 95-105, Kluwer Academic Publishers, London, 2002.

⁷Siddiqi, A., Alsan, S., Rasulov, M., Oğuz, O. and Aslan Z., "International workshop on applications of wavelets to real world problems: IWW2005", July 17-18, ISBN: 975-6516-11-9, ITICU Publication No: 12, Istanbul, 2005, p.290.

⁸www.ucar.edu/communications/factsheets/el_nino/Figure_5.html

⁹www.cpc.noaa.gov/products/precip/CWlink/daily_ao_index/history/methods.html

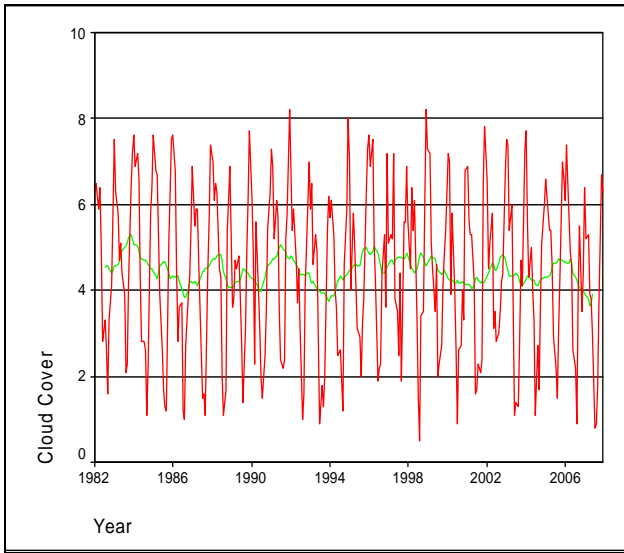
¹⁰www.ssa.org/files/member/Methodology.pdf

Table 1
Definitions of climate variability

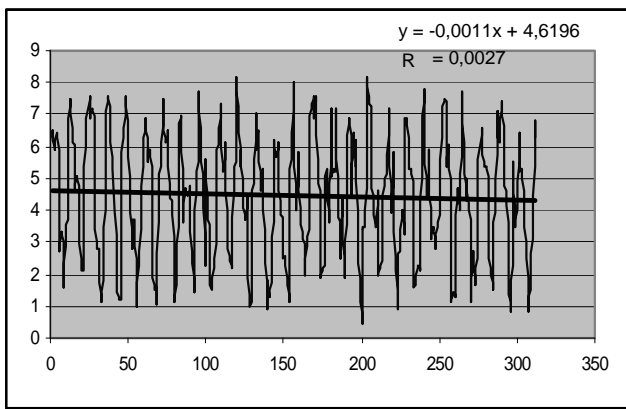
Climate Variability	Time Scale
Inter-monthly fluctuations	2.0-3.1 months
Semi-annual cycle	4.7-7.4 months
Residual annual cycle	1.3-16.0 months
Inter-annual variations	2.2-3.5 years
Sub-decadal variations	5.3-8.3 years
Decadal to centennial changes	10.6-110.7 years



Figure 1 The locations of the stations in Turkey.

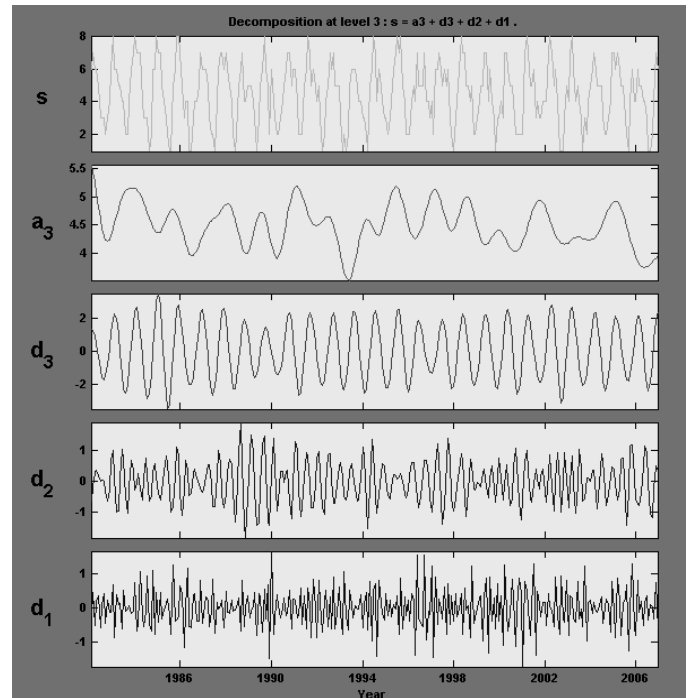


a)

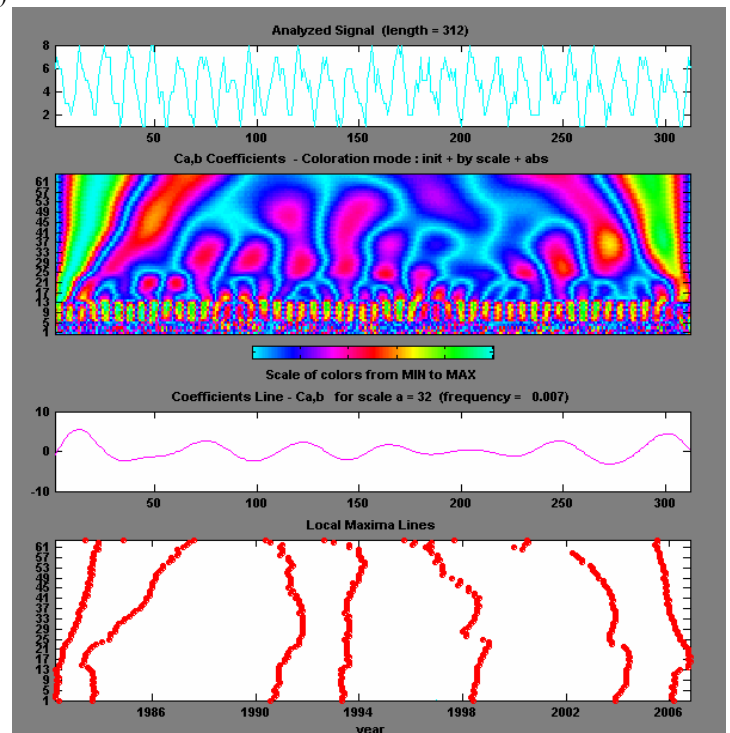


b)

Figures 2a, 2b Temporal variation of cloud cover (0 = clear and 10 = overcast) in Eskişehir between (1982-2007), (a) moving averages for lag = 12, (b) linear trend (the sequence number: 1 = January 1982 and 305 = December 2007).



c)



d)

Figures 2c, 2d Wavelet analysis of cloud cover values in Eskişehir between 1982 and 2007, (c) 1D wavelet analysis DMeyer, Period 3; s: signal, a3: approximation, d1-d3: details at three levels (d) 1D continuous wavelet analysis, DMeyer, Level 3.(1 < freq. < 61 months).

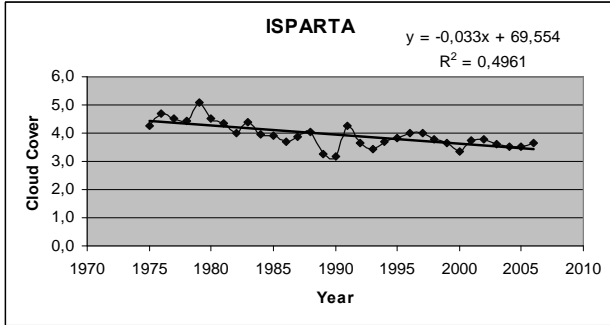


Figure 3a Annual variation of cloud cover values in Isparta (1975-2006, $\alpha = 0,01$).

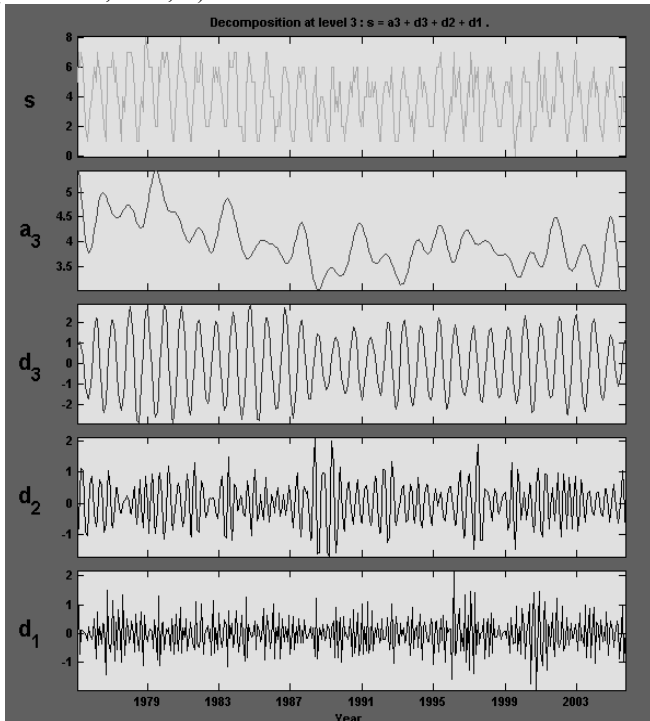


Figure 3b 1D wavelet analysis of cloud cover values in Isparta.

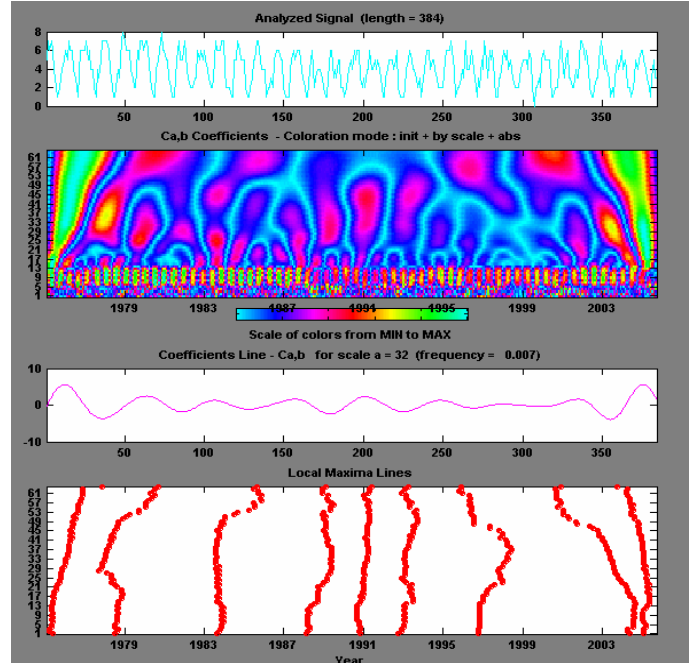


Figure 3c Monthly variation of 1D continuous wavelet of cloud cover values at Isparta (1975-2006), DMeyer, Level 3. (1 <freq. <61 months, first part of the figure shows raw signal (CC), second part shows 1D continuous wavelet at different scales, third and fourth graphs represents local maxima).

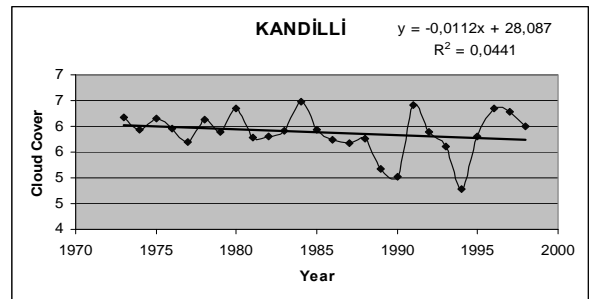


Figure 4a Annual average cloud cover values in Kandilli (1973-1996)

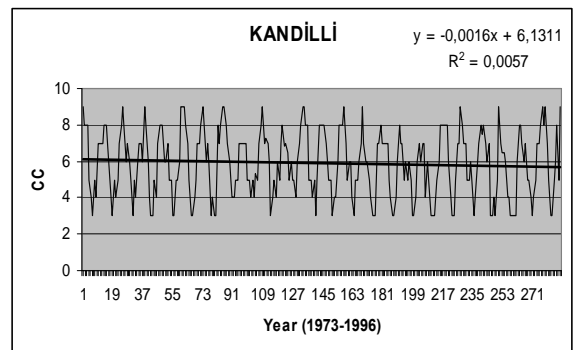


Figure 4b Monthly average values of cloud cover (CC) variations at Kandilli (1973-1996).

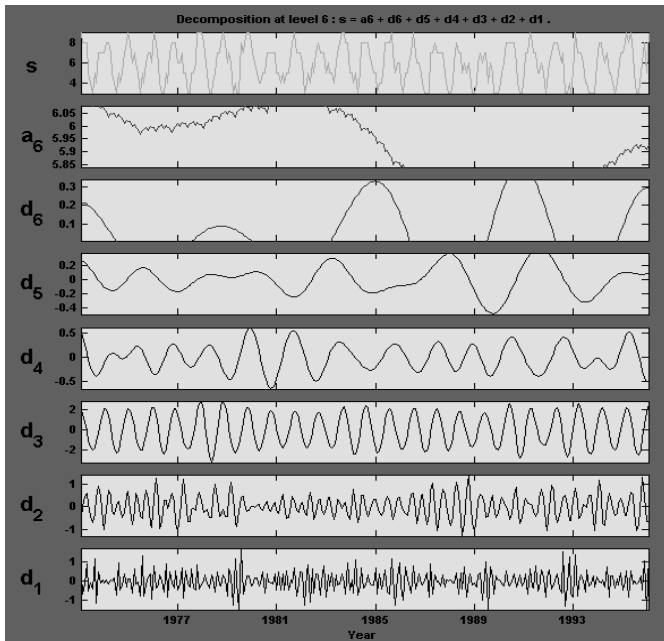


Figure 4c 1D wavelet analysis of cloud cover values at Kandilli (1973-1996), DMeyer, Sampling Period 6, (s: signal (CC), a_6 : approximation, d_1 - d_6 : details at six levels).

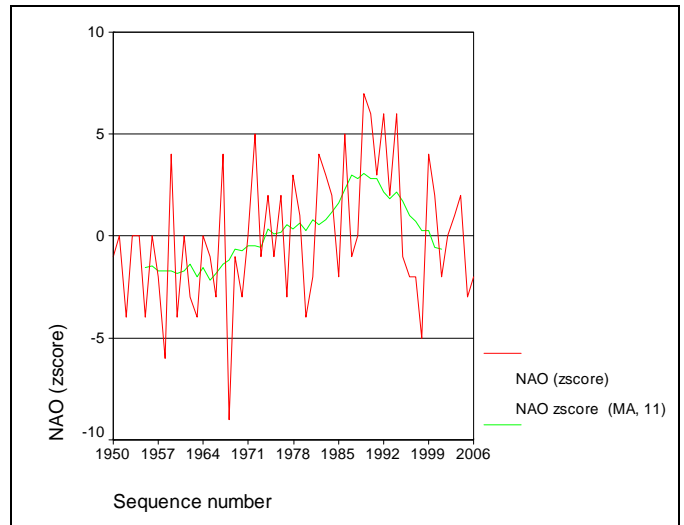


Figure 5a Temporal variation and moving averages of NAO z-scores between 1950 and 2006, (lag=11 months).

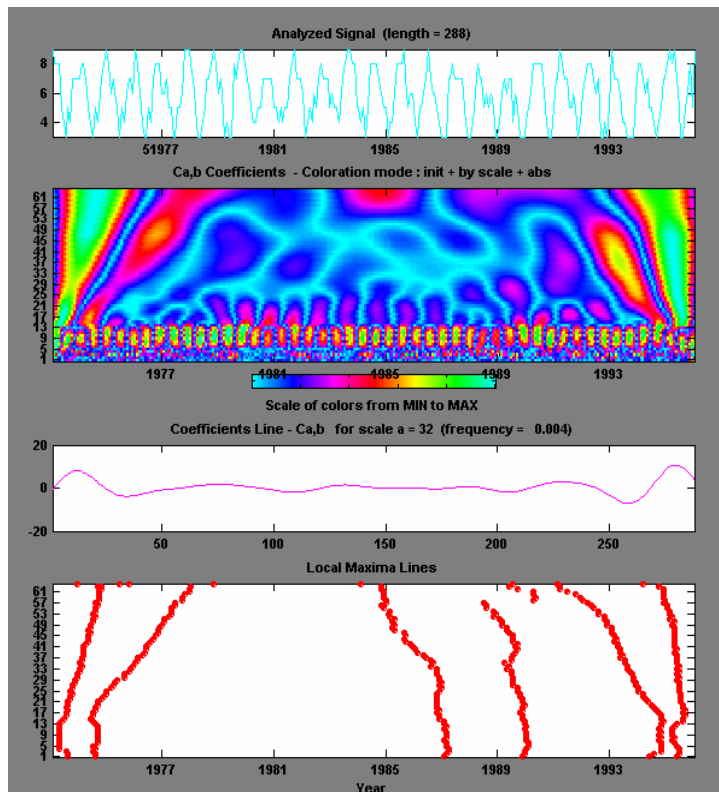


Figure 4d Monthly variation of 1D continuous wavelet of cloud cover values at Kandilli (1973-1996), DMeyer, Sampling Period 6, (raw signal, 1D continuous wavelet and local maxima lines).

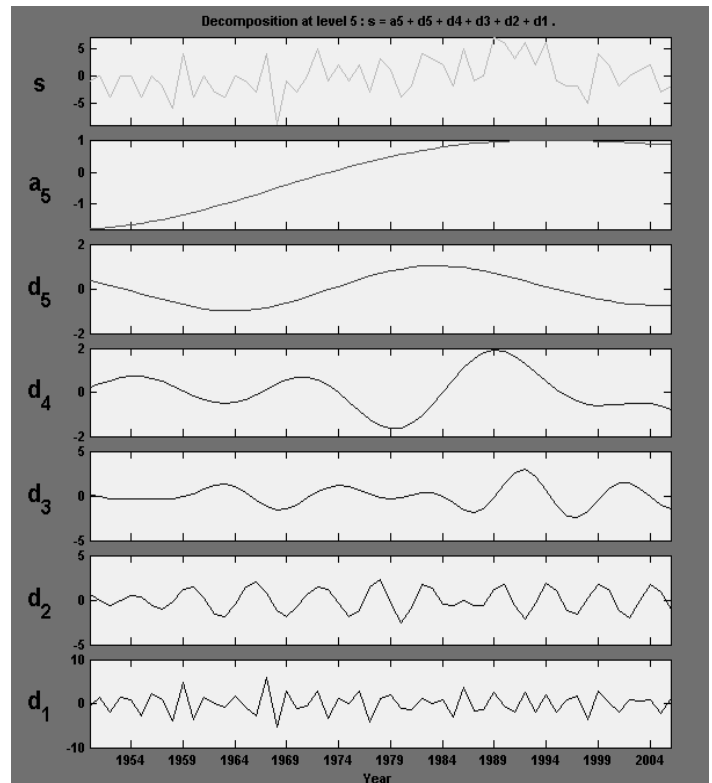


Figure 5b NAO z-score, 1D Wavelet, DMeyer, Level 5, (s: signal, a_5 : approximation, d_1 - d_5 : details at 5 levels).

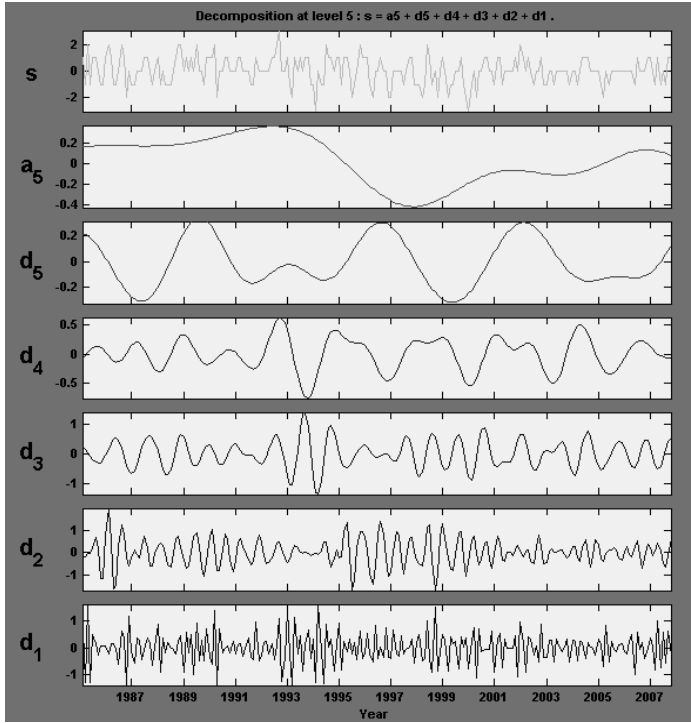


Figure 5c NAO z-score, 1D Wavelet, DMeyer, Period 5, (s: signal, a5: approximation, d1-d5 details at different levels).

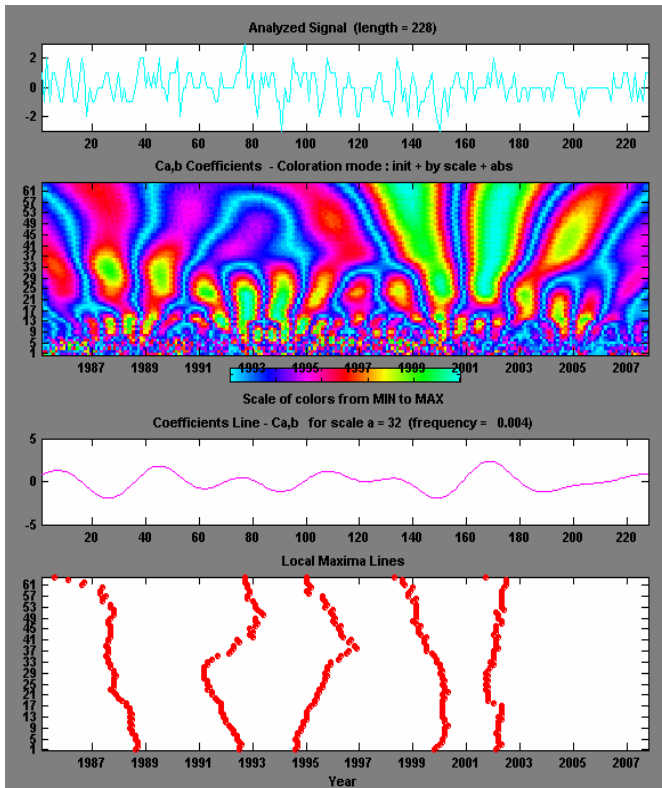
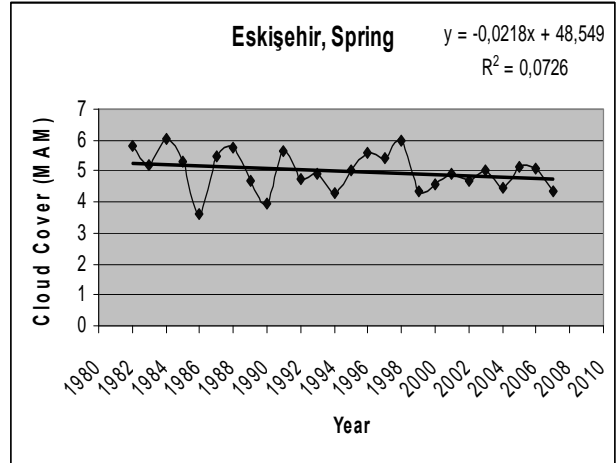
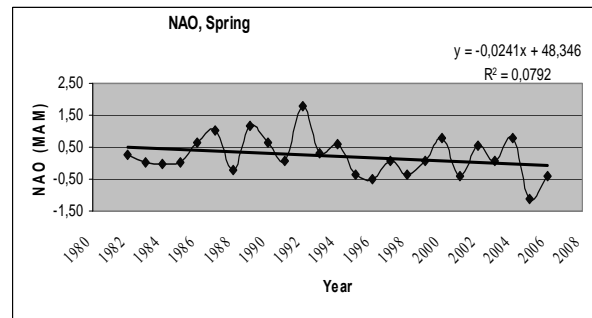


Figure 5d Continuous wavelet NAO Z-scores, 1986-2004, DMeyer, Level, (s: signal, 1 < frequency < 61months, local maxima).

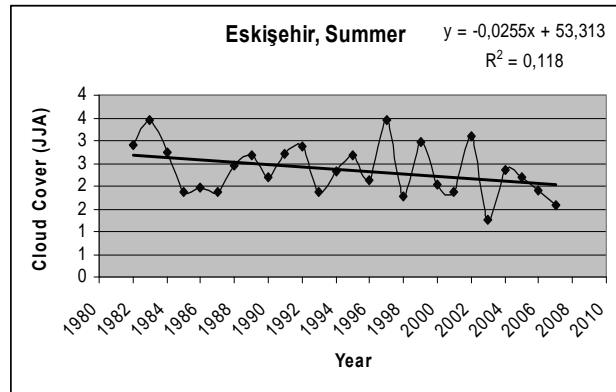


a)

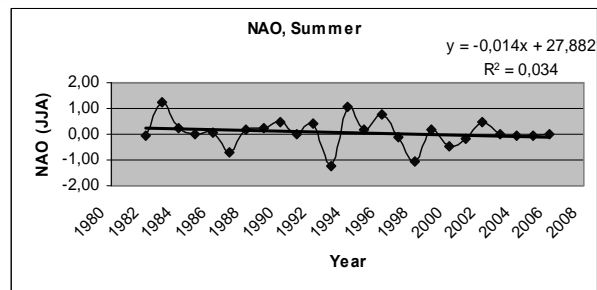


b)

Figures 6a, 6b a) Variations of cloud cover in spring in Eskişehir between 1982 - 2006 and b) the corresponding averages of NAO.

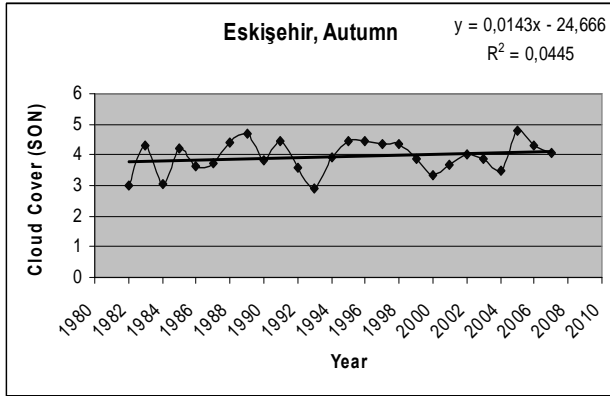


c)

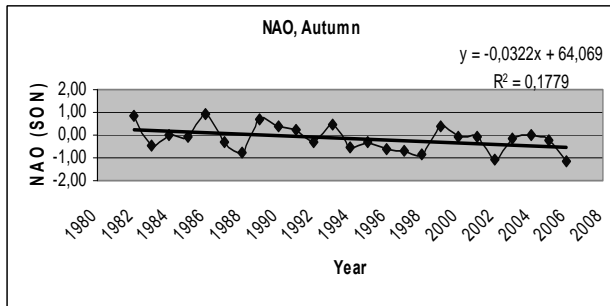


d)

Figure 6c, d c) Variations of cloud cover in summer in Eskişehir between 1982 - 2006 and d) the corresponding averages of NAO.



e)



f)

Figure 6e, f e) Variations of cloud cover in autumn in Eskişehir between 1982 - 2006 and f) the corresponding averages of NAO, ($\alpha=0,05$).

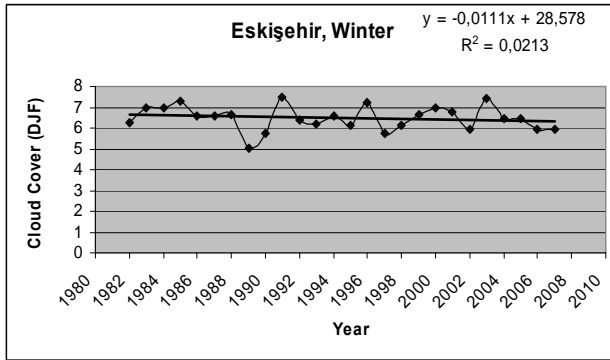


Figure 6g Variations of cloud cover in winter in Eskişehir between (1982 – 2006)

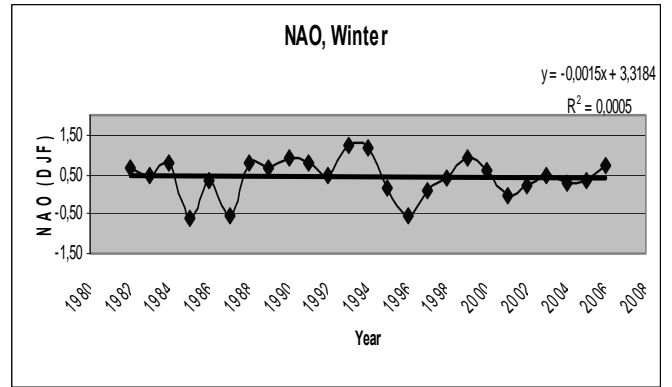
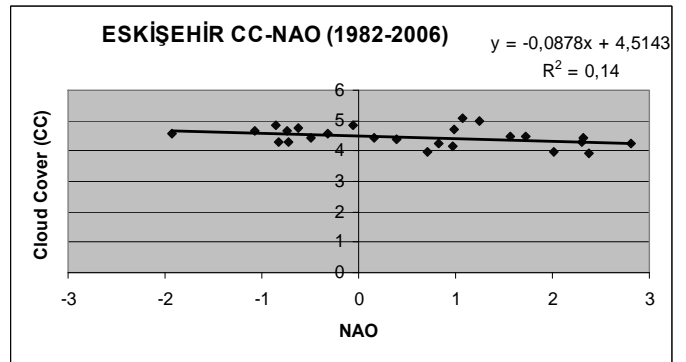
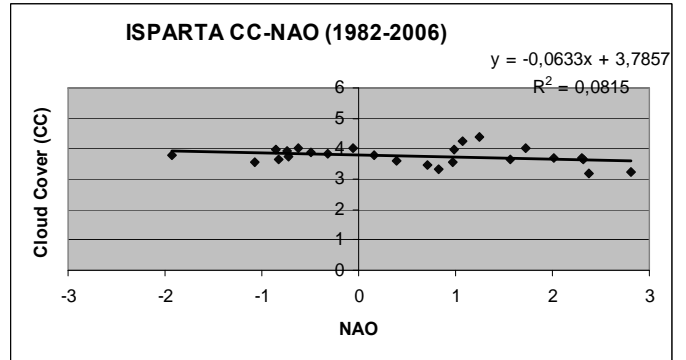


Figure 6h Variations of NAO (1982-2006).



i)



j)

Figures 6i, 6j i) Linear relation between annual cloud cover averages and NAO values, in Eskişehir, j) in Isparta between 1982 – 2006.